Circulation
Arrhythmia and Electrophysiology

American Heart Association®

Evaluation of the Necessity for Cardioverter-Defibrillator Implantation in Elderly Patients With Brugada Syndrome

Tsukasa Kamakura, Mitsuru Wada, Ikutaro Nakajima, Kohei Ishibashi, Koji Miyamoto, Hideo Okamura, Takashi Noda, Takeshi Aiba, Hiroshi Takaki, Satoshi Yasuda, Hisao Ogawa, Wataru Shimizu, Takeru Makiyama, Takeshi Kimura, Shiro Kamakura and Kengo Kusano

Circ Arrhythm Electrophysiol. 2015;8:785-791; originally published online June 11, 2015;
doi: 10.1161/CIRCEP.114.002705
Circulation: Arrhythmia and Electrophysiology is published by the American Heart Association, 7272 Greenville Avenue, Dallas, TX 75231

Print ISSN: 1941-3149. Online ISSN: 1941-3084

PLOS | ONE

RESEARCH ARTICLE

Exome Analyses of Long QT Syndrome Reveal Candidate Pathogenic Mutations in Calmodulin-Interacting Genes

Daichi Shigemizu[1☯‡], Takeshi Aiba[2☯‡], Hidewaki Nakagawa[3], Kouichi Ozaki[4], Fuyuki Miya[1], Wataru Satake[5], Tatsushi Toda[5], Yoshihiro Miyamoto[6], Akihiro Fujimoto[3], Yutaka Suzuki[7], Michiaki Kubo[8], Tatsuhiko Tsunoda[1], Wataru Shimizu[2,9]*, Toshihiro Tanaka[4,10]*

1 Laboratory for Medical Science Mathematics, RIKEN Center for Integrative Medical Sciences, Yokohama, Japan, **2** Department of Cardiovascular Medicine, National Cerebral and Cardiovascular Center, Suita, Japan, **3** Laboratory for Genome Sequencing Analysis, RIKEN Center for Integrative Medical Sciences, Yokohama, Japan, **4** Laboratory for Cardiovascular Diseases, RIKEN Center for Integrative Medical Sciences, Yokohama, Japan, **5** Division of Neurology/Molecular Brain Science, Kobe University Graduate School of Medicine, Kobe, Japan, **6** Department of Preventive Cardiology, National Cerebral and Cardiovascular Center, Suita, Japan, **7** Department of Computational Biology, Division of Biosystem Sciences, University of Tokyo, Chiba, Japan, **8** Laboratory for Genotyping Development, RIKEN Center for Integrative Medical Sciences, Yokohama, Japan, **9** Department of Cardiovascular Medicine, Nippon Medical School, Tokyo, Japan, **10** Department of Human Genetics and Disease Diversity, Tokyo Medical and Dental University Graduate School of Medical and Dental Sciences, Tokyo, Japan

☯ These authors contributed equally to this work.
‡ These authors are co-first authors on this work.
* wshimizu@nms.ac.jp (WS); toshitan@src.riken.jp (TT)

Citation: Shigemizu D, Aiba T, Nakagawa H, Ozaki K, Miya F, Satake W, et al. (2015) Exome Analyses of Long QT Syndrome Reveal Candidate Pathogenic Mutations in Calmodulin-Interacting Genes. PLoS ONE 10(7): e0130329. doi:10.1371/journal.pone.0130329

Academic Editor: Alvaro Galli, CNR, ITALY

Received: January 10, 2015

Accepted: May 19, 2015

Published: July 1, 2015

Data Availability Statement: Some access restrictions apply to the data underlying the findings. All data relevant for the interpretation of our findings are provided in the paper or the supplementary information, except for the raw sequence data. Genetic data are considered as personal private data in Japan, therefore we are not allowed to submit to a public repository. All mutations in known LQTS genes and in candidate genes, identified in this study, have been deposited into NCBI ClinVar with the accession numbers SCV000221974 - SCV000222093.

Funding: Drs. W. Shimizu, TA, YM, and T. Tanaka were supported in part by the Research Grant for the

Abstract

Long QT syndrome (LQTS) is an arrhythmogenic disorder that can lead to sudden death. To date, mutations in 15 LQTS-susceptibility genes have been implicated. However, the genetic cause for approximately 20% of LQTS patients remains elusive. Here, we performed whole-exome sequencing analyses on 59 LQTS and 61 unaffected individuals in 35 families and 138 unrelated LQTS cases, after genetic screening of known LQTS genes. Our systematic analysis of familial cases and subsequent verification by Sanger sequencing identified 92 candidate mutations in 88 genes for 23 of the 35 families (65.7%): these included eleven *de novo*, five recessive (two homozygous and three compound heterozygous) and seventy-three dominant mutations. Although no novel commonly mutated gene was identified other than known LQTS genes, protein-protein interaction (PPI) network analyses revealed ten new pathogenic candidates that directly or indirectly interact with proteins encoded by known LQTS genes. Furthermore, candidate gene based association studies using an independent set of 138 unrelated LQTS cases and 587 controls identified an additional novel candidate. Together, mutations in these new candidates and known genes explained 37.1% of the LQTS families (13 in 35). Moreover, half of the newly identified candidates directly interact with calmodulin (5 in 11; comparison with all genes; p=0.042). Subsequent variant analysis in the independent set of 138 cases identified 16 variants in the 11 genes, of which 14 were in calmodulin-interacting genes (87.5%). These

Cardiovascular Diseases (H24-033, H26-040) from the Ministry of Health, Labour and Welfare, Japan. The funders had no role in study design, data collection and analysis, decision to publish, or preparation of the manuscript.

Competing Interests: The authors have declared that no competing interests exist.

results suggest an important role of calmodulin and its interacting proteins in the pathogenesis of LQTS.

Introduction

Long QT syndrome (LQTS) is characterized by a prolonged QT interval in the electrocardiogram (ECG) and ventricular tachyarrhythmia. Arrhythmia is often triggered by exercise, particularly swimming, or emotional stress, resulting in recurrent syncope, seizures, and sometimes, sudden, unexpected cardiac death [1].

LQTS has an estimated prevalence as high as one in 2,000 people [2]. To date, mutations in 15 susceptibility genes have been identified. The majority of those affected have mutations in *KCNQ1* (LQT1), *KCNH2* (LQT2) and *SCN5A* (LQT3), encoding potassium and sodium ion channel alpha-subunits. These three genes account for 75% of LQTS cases (LQT1: 30%-35%, LQT2: 25%-30%, LQT3: 5%-10%), while the remaining known LQTS genes, which encode beta subunits of plasma membrane channels, channel-interacting proteins, structural membrane scaffolding proteins or membrane anchoring proteins, account for only 5% of cases [3]. Mutations have not been detected in the remaining 20% of patients.

Whole-exome sequencing (WES) is widely used to identify genetic variations in coding regions [4]. WES is more powerful and cost-effective for exonic regions than whole-genome sequencing because it obtains a deeper coverage of the target regions. WES has been recently used to successfully identify causal mutations of Mendelian diseases [5, 6] and driver mutations in tumors [7–9].

Here, we report the identification of candidate pathogenic mutations, through WES and validated by Sanger sequencing, in two-thirds of the examined LQTS families. Although no commonly mutated gene was identified other than known genes, protein-protein interaction (PPI) network analysis revealed that ten candidates interact with proteins encoded by known LQTS genes. Interestingly, half of these directly interact with calmodulin, which is statistically significant when compared to the number of molecules that directly interact with calmodulin. In addition, candidate gene based association studies using an independent set of unrelated LQTS individuals and unaffected individuals identified an additional novel LQTS candidate. Examination of the presence of mutations in these candidate genes in the unrelated LQTS cases revealed that most mutations were in calmodulin-interacting genes. We believe these findings contribute to a greater understanding of LQTS and provide clues for future research into its pathogenic mechanism.

Materials and Methods

Ethics Statement

This study was approved by the ethics committee of the Institutes of National Cerebral and Cardiovascular Center and RIKEN. The design and performance of the current study involving human subjects were clearly described in a research protocol. All participants provided written informed consent before taking part in this research.

Study subjects

LQTS is diagnosed using the following criteria: patients with a Schwartz risk score > 3.5 in the absence of a secondary cause for QT prolongation [10], and/or an unequivocally pathogenic

mutation in one of the LQTS genes, or QTc > 500 ms in repeated 12-lead ECG in the absence of a secondary cause for QT prolongation. Among the LQTS patients registered at National Cerebral and Cardiovascular Center who provided written informed consent, we recruited 186 genetically unrelated LQTS cases whose mutations were not detected by genetic screening of known LQTS genes. Among them, 35 had family data (21 family trio data of LQTS patients with unaffected parents and 14 pedigrees with at least one additional LQTS family member, S1 Fig) with DNA samples, and therefore were selected for pedigree analysis. Therefore, among the 35 families, excluding the proband, an additional 85 family members (24 LQTS and 61 unaffected control subjects) were recruited for this analysis. We also included the remaining 151 samples with no family data as genetically independent LQTS cases. In total, 271 samples were subjected to WES analysis. In the course of the analysis, we detected mutations in known LQTS genes for 13 out of 151 non-pedigree cases (Table 1) [11–14] and these individuals were excluded from further analysis. Consequently, we examined 59 LQTS and 61 unaffected individuals in 35 families and 138 unrelated LQTS cases (n = 258). The participant summary, including gender, average age, and the other clinical information, is shown in Table 2.

Whole-exome sequencing

Exome capture was performed by the Agilient SureSelect Human All Exon V4 according to the manufacturer's instructions. This kit captures genomic DNA by in-solution hybridization with RNA oligonucleotides, enabling specific targeting of approximately 51Mb of the human genome. The captured DNA was sequenced using the Illumina HiSeq2000 platform with paired-end reads of 101bp for insert libraries of 150–200bp according to the manufacturer's instructions.

Exome sequence data analysis

Read sequences were mapped by the Burrows-Wheeler Aligner (BWA: version 0.6.1) [15] to the human reference genome (GRCh37). Duplicate PCR reads were identified and removed using SAMtools (version 0.1.8) [16] and in-house software. After filtering by pair mapping distance, mapping uniqueness and pair orientation, the mapping result files were converted into pileup format using SAMtools. Variant calling was conducted based on methods we have published elsewhere, VCMM [17]. We used the following quality control filters: (i) alignments near putative indels were refined using GATK [18]; (ii) a stand bias filter excluded variants whose alternative allele was preferentially found in one of the two available read orientations at the site.

Variants that were found in dbSNP (version 137) [19], 1000 Genomes Project (n = 1,094) [20], NHLBI Exome Sequencing Project Exome Variant Server (n = 6,503; http://evs.gs.washington.edu/EVS/) [accessed June 2012] (ESP6500) [21] and our in-house whole genome and exome data composed of 1,257 non-cardiac Japanese individuals were excluded from further analyses. Nongenic, intronic and synonymous variants other than those occurring at canonical splice sites and non-synonymous variants predicted as benign/tolerant by both SIFT (http://sift.jcvi.org/www/) [22] and PolyPhen-2 (http://genetics.bwh.harvard.edu/pph2/) [23] were also excluded. Furthermore, we assumed that affected individuals had *de novo* or recessive (both homozygous and compound heterozygous) mutations for parent/affected offspring trio families and dominant for the other families. All candidate mutations were validated using Sanger sequencing of both the affected and unaffected individuals.

All mutations in known LQTS genes and in candidate genes, identified in this study, have been deposited into NCBI ClinVar with the accession numbers SCV000221974—SCV000222093.

Table 1. Identification of known-gene and disease-causing variant in the LQTS.

Phenotype	Gene symbol	Transcript ID	cDNA level change	Protein level change	QTc (ms)	Symptoms	HGMD†, others
LQT1*	*KCNQ1*	NM_000218.2	c.760G>A	p.V254M	570	syncope	CM960898 [11]
LQT1*	*KCNQ1*	NM_000218.2	c.965C>T	p.T322M	474	asympt	CM057152 [12]
LQT1	*KCNQ1*	NM_000218.2	c.683+2T>G	-	470	Asymp	Pedigree analysis
LQT1	*KCNQ1*	NM_000218.2	c.1032+1G>A	-	572	TdP VF Sym40yo	Pedigree analysis
LQT2*	*KCNH2*	NM_000238.3	c.1849T>C	p.F617L	475	asympt	
LQT2*	*KCNH2*	NM_000238.3	c.1831T>G	p.Y611D	490	VF	CM107399 [13]
LQT2*	*KCNH2*	NM_000238.3	c.307+2T>A	-	548	asympt	
LQT3*	*SCN5A*	NM_001160160.1	c.4900G>A	p.V1634I	448	TdP	
LQT4*	*ANK2*	NM_001148.4	c.2474C>T	p.T825I	436	syncope	
LQT4*	*ANK2*	NM_001148.4	c.4876A>G	p.K1626E	650	syncope	
LQT4*	*ANK2*	NM_001148.4	c.6149T>C	p.I2050T	464	VF	
LQT4*	*ANK2*	NM_001148.4	c.8123T>C	p.V2708A	420	asympt	
LQT5	*KCNE1*	NM_000219.3	c.253G>A	p.D85N	492	asympt	CM040436 [14], Pedigree analysis, rare variant
LQT9	*CAV3*	NM_033337.2	c.37A>T	p.I13F	466	asympt	Pedigree analysis, SNV
LQT11*	*AKAP9*	NM_147185.2	c.2295T>A	p.D765E	453	asympt	
LQT11*	*AKAP9*	NM_147185.2	c.5341T>A	p.S1781T	457	asympt	
LQT12*	*SNTA1*	NM_003098.2	c.1498C>T	p.R500C	444	asympt	
	NOS1AP	NM_014697.2	c.1276G>A	p.V426M	413	asympt	disease causing variant
	NOS1AP	NM_014697.2	c.824C>T	p.S275F	453	syncope	disease causing variant

asympt; asymptomatic, SNV: single nucleotide variant

†accession number obtained from HGMD professional (ver. 2014.4, accessed on Mar. 19, 2015)

*mutations detected in known LQTS genes for non-pedigree cases.

doi:10.1371/journal.pone.0130329.t001

Network analysis

Network analysis was performed using the Ingenuity Pathway Analysis software (IPA; Ingenuity Systems) based on the 15 known LQTS genes and the 88 candidate pathogenic genes identified. We considered molecules and/or relationships available in the IPA Knowledge Base for human, mouse and rat and set the confidence filter to experimentally observed or high (predicted). Networks were generated with a maximum size of 35 genes and allowing up to 10 networks. Molecules in the query set with recorded interactions were eligible for network

Table 2. Clinical background of LQTS patients and their family members.

	35 LQTS families		unrelated LQTS (n = 138)
	LQTS (n = 59)	Control (n = 61)	
age	23±18	25±18	19±16
male/ female	20/39	36/25	54/84
QTc (ms)	480±40	402±21	466±49
syncope, n (%)	24 (41)	1 (1)	59 (43)
VF or CA, n (%)	9 (15)	0 (0)	18 (13)

VF: ventricular fibrillation, CA: cardiac arrest

doi:10.1371/journal.pone.0130329.t002

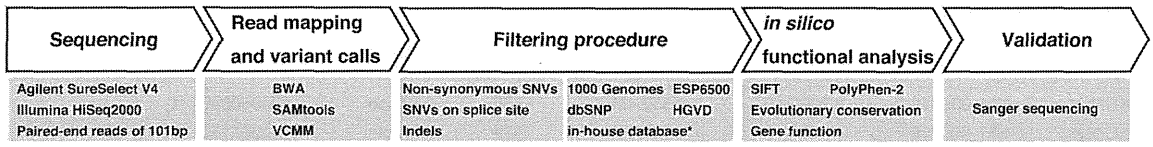

Fig 1. Experimental work flow for detecting sequence variants by WES. In-house database with asterisk is our in-house whole exome or whole genome data composed of 1,257 non-cardiac Japanese individuals.

doi:10.1371/journal.pone.0130329.g001

construction using the IPA algorithm. Networks were ranked by IPA network score according to their degree of relevance to the eligible molecules in the query data set. The network score is calculated using Fisher's exact test on a basis of the number of eligible molecules in the network and its size, as well as the total number of eligible molecules analyzed and the total number of molecules in the Ingenuity Knowledge Base that could potentially be included in the networks.

Quality control and gene-based association study

We used 748 Japanese individuals, which included 161 LQTS cases (23 probands in LQTS families and 138 independent LQTS patients) and 587 controls. Closely related subjects, where the identity-by-descent (IBD) proportion of alleles shared was over 0.125, and outliers by principal-component analysis (PCA) [24] (S2 Fig) were previously excluded. We estimated the IBD sharing score using PLINK's '-genome' option [25] and performed PCA using *gdsfmt* and *SNPRelate* packages in the statistical software R [26]. We also excluded all SNVs with a genotype call rate < 0.80, a Hardy-Weinberg equilibrium p-value $< 1\times10^{-6}$ or nongenic and intronic variants other than those occurring at canonical splice sites. When also considering a MAF < 0.005, 51,393 SNVs passed these stringent quality control criteria. The quantile-quantile (QQ) plots of the p-values from the Cochran-Armitage test for trend showed the genomic inflation factor λ_{GC} to be 1.027 (S3 Fig).

For the gene-based association studies, we used the SKAT-O test [27], which encompasses both burden tests (e.g. CMC method [28]) and variance-component tests (e.g. SKAT [29]). We performed the analysis using default weights and MAF < 0.01 for the combination of non-synonymous variants predicted to be damaging by SIFT [22] or PolyPhen-2 [23] analysis and splice-site variants. We performed the test for candidate genes with at least two variants and declared a gene-based test association significant when q-value < 0.05.

Results

Identification of candidate mutations in probands

On average, 6.7 Gbp of short read sequence data were obtained from WES (S1 Table). In total, 68.6% of the sequenced bases were mapped to the targeted regions and 92.8% of mapped exon sequences had at least ten times coverage (S4 Fig). The average coverage was 68X across individuals. An average of 19,505 coding SNVs and 516 coding insertion/deletion (indels) were identified per proband with high confidence (S2 Table). We developed an automated pipeline to systematically identify all candidate non-synonymous mutations in each affected individual (Fig 1). We first excluded all synonymous variants other than those occurring at canonical splice sites. This first step reduced the number of candidates to an average of 9,256 non-synonymous and canonical splice site variants per proband. We further reduced this number to 76 variants and 15 coding indels by excluding variants found in public databases; dbSNP137 [19], 1000 Genomes Project [20], NHLBI Exome Variant Server (ESP6500) [21], the Human Genetic Variation Database (HGVD: http://www.genome.med.kyoto-u.ac.jp/SnpDB). We also used

our in-house whole exome or whole genome database composed of 1,257 Japanese individuals. We then excluded the variants predicted as benign/tolerant by both SIFT (http://sift.jcvi.org/www/) [22] and PolyPhen-2 (http://genetics.bwh.harvard.edu/pph2/) [23], and finally selected candidate mutations that co-segregated among affected individuals within each of the pedigrees (S2 Table). We identified 92 candidate pathogenic mutations in 88 genes in 23 out of the 35 families (65.7%), all of which were validated by Sanger sequencing. These are eleven *de novo*, five recessive (two homozygous and three compound heterozygous) and seventy-three dominant mutations (S3 Table). No gene was found to be commonly mutated among pedigrees.

Protein-protein interaction (PPI) network analysis

We applied PPI network analysis to a gene set of the 15 known genes and the 88 candidate pathogenic genes identified in this analysis, in order to elucidate any enrichment of functional units or categories. Using Ingenuity Pathways analysis software (IPA; Ingenuity Systems), we identified an interesting network, ranked top in IPA network score, composed of proteins encoded by all 15 known genes and 10 candidate pathogenic genes. Seven of the 10 pathogenic candidates were found to directly interact with at least one protein encoded by known LQTS genes (Fig 2) and contain candidate mutations that occur at evolutionarily conserved amino acids (S5 Fig) which were predicted to be damaging by SIFT [22] or PolyPhen-2 [23] analysis and to have a strong functional impact on the gene (Table 3). In addition, half of the 10 pathogenic candidates were calmodulin-interacting genes (*RYR2*, *UBR4*, *UBR5*, *PI4KA* and *KIF21B*) (Fig 2), which was statistically significant when compared to the number of molecules that directly interact with calmodulin ($p = 0.042$, Fisher's exact test). We previously reported that calmodulin mutations are associated with LQTS [30]. These results suggest an important role of calmodulin and its interacting proteins in the pathogenesis of LQTS. Through PPI analysis, we could detect candidate mutations in 12 families.

Candidate gene-based association study using an independent set of case/control samples

We could not identify candidate pathogenic genes supported by PPI analysis for the remaining 11 families, although 44 genes were still candidates. Therefore, we performed candidate gene-based association studies using the sequence kernel association optimal test: SKAT-O (Fig 3, see Materials and Methods) [27], in order to identify likely pathogenic genes with cumulative effects in LQTS patients from the 44 candidate genes. We used 11 probands from each of these families, 12 probands from each of the families in which no candidates were identified by pedigree analysis, and a set of 138 genetically unrelated LQTS cases and 587 controls (Fig 3). In total, 161 cases and 587 controls were examined and a significant association in the *SLC2A5* gene (also known as *GLUT5*, FDR-adjusted p-value (q-value) = 0.014, Tables 3 and 4) was found.

Candidate pathogenic mutations in an independent set of unrelated LQTS cases

Investigation into the presence of possible mutations in these 11 genes in 138 genetically independent cases identified 16 candidate pathogenic mutations in 15 individuals (Table 5, candidate mutations in both *WDR26* and *RYR2* were identified in the same individual), which were non-synonymous variants and absent from in-house/public variant databases. Out of the 16 candidate mutations, 14 were calmodulin-interacting genes (87.5%, Fig 2), and 9 of these

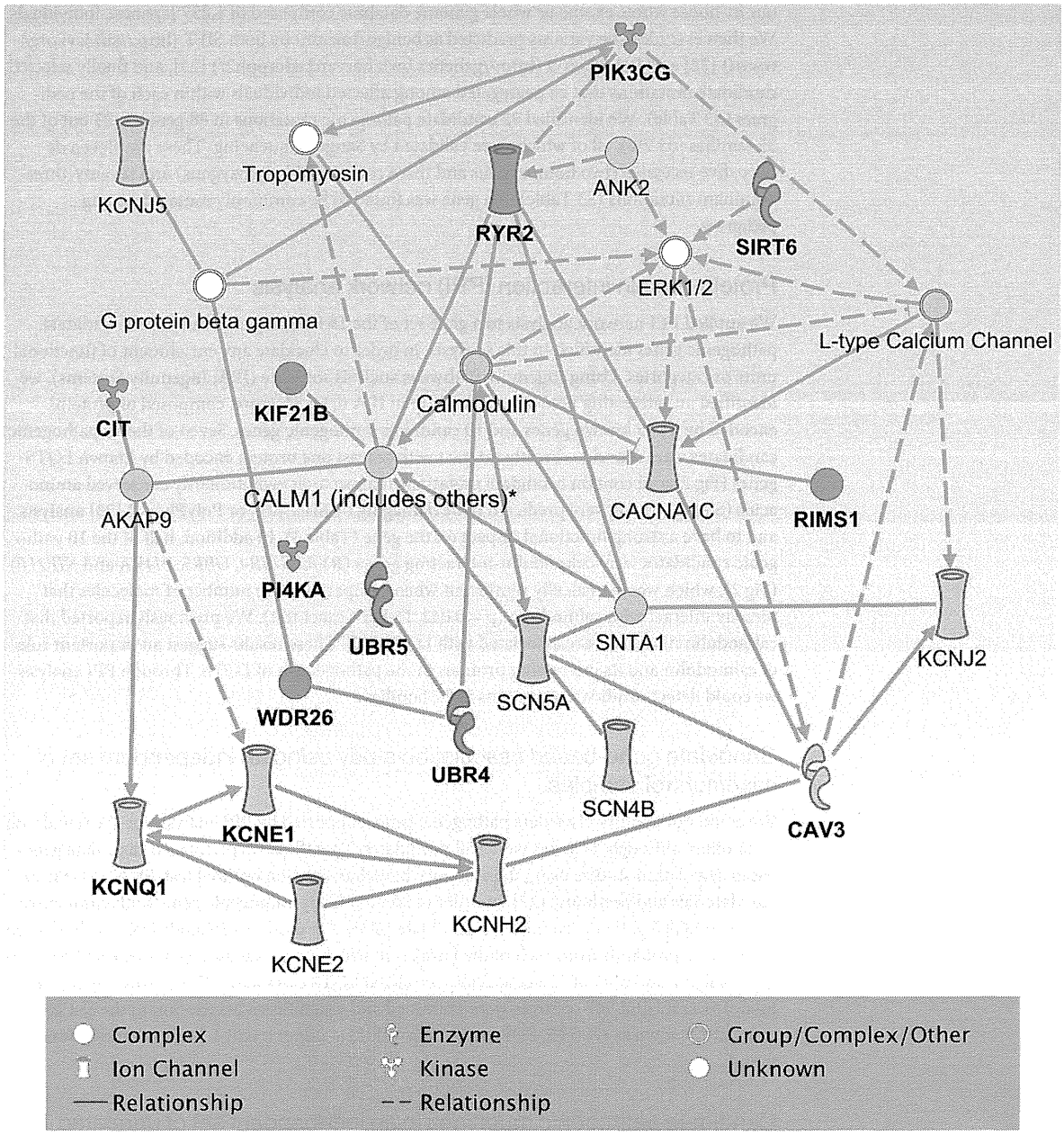

Fig 2. The top-scoring IPA network constructed on the basis of known genes/proteins and candidate pathogenic genes/proteins identified. The green and pink objects represent known LQTS genes and candidate pathogenic genes identified in this PPI analysis, respectively.

doi:10.1371/journal.pone.0130329.g002

Table 3. Potential pathogenic mutations detected in PPI analysis and Gene based Association Study (GAS) using independent samples.

ID	Gene	Model†	Transcript ID	cDNA level change	Protein level change	SIFT/PolyPhen-2*	Analysis
T02	*WDR26*	*De novo*	NM_025160.6	c.612G>T	p.L204F	T/-	PPI
T08	*RYR2*	*De novo*	NM_001035.2	c.12272C>T	p.A4091V	D/D	PPI
T12	*UBR5*	AR (CHTZ)	NM_015902.5	c.5837A>G	p.H1946R	D/P	PPI
				c.3752G>A	p.R1251H	D/B	PPI
T17	*UBR4*	*De novo*	NM_020765.2	c.6397G>A	p.A2133T	T/D	PPI
T21	*KIF21B*	*De novo*	NM_017596.2	c.3601C>T	p.R1201W	D/D	PPI
D02	*SLC2A5*	AD	NM_003039.2	c.808C>T	p.R270W	D/D	GAS
D03	*CIT*	AD	NM_001206999.1	c.5786C>A	p.S1929Y	D/D	PPI
D04	***KCNQ1***	AD	NM_000218.2	c.683+2T>G	-	-/-	PPI
D07	***CAV3***	AD	NM_033337.2	c.37A>T	p.I13F	T/B	PPI
D08	***KCNQ1***	AD	NM_000218.2	c.1032+1G>A	-	-/-	PPI
D09	***KCNE1***	AD	NM_000219.3	c.253G>A	p.D85N	D/P	PPI
D10	*SIRT6*	AD	NM_016539.2	c.742C>T	p.R248C	D/D	PPI
	PIK3CG	AD	NM_002649.2	c.574G>A	p.D192N	T/D	PPI
D14	*PI4KA*	AD	NM_058004.2	c.247G>A	p.D83N	D/D	PPI
	RIMS1	AD	NM_014989.4	c.1477G>C	p.E493Q	D/D	PPI

*D = damaging; P = probably damaging; T = tolerated; B = benign.

†AR: autosomal recessive (CHTZ = compound heterozygous), AD: autosomal dominant. Bold: known LQTS genes.

doi:10.1371/journal.pone.0130329.t003

occurred at evolutionarily conserved amino acids (64.3%): four were missense variants in *RYR2*, three in *UBR4*, one in *PI4KA* and one in *KIF21B* (Table 5). Functional analysis of these mutations though evolutionarily conserved amino acid residue examination showed these mutations to be strong candidates.

Interestingly, nine (including 6 novel) mutations were identified in the *RYR2* gene, which were found in younger patients with no affected family members (Table 6). Many of the patients with the *RYR2* mutation had similar exercise-induced cardiac events (4 syncope, 2 VF, 1 cardiac arrest). This frequency was also higher and more severe compared with that in genotype-unknown LQTS, while the QTc interval was shorter in patients with the *RYR2* mutation than that with genotype-negative LQTS (439 ± 30 vs. 471 ± 50 ms; p-value = 0.01), strengthening the importance of *RYR2* in LQTS pathogenesis.

Discussion

We sequenced the exomes of 59 LQTS individuals and 61 unaffected individuals from 35 families and systematically identified candidate mutations in the affected individuals. Subsequent PPI network analysis revealed that a statistically significant proportion of pathogenic candidate molecules interacted directly with calmodulin (*RYR2* [31], *UBR4* [32], *UBR5* [33], *PI4KA* [34] and *KIF21B* [34]). Calmodulin is a primary sensor of intracellular calcium levels in eukaryotic cells, playing a key role in the proper mediation of Ca^{2+} signaling, and interacts with several known LQTS genes (*SCN5A* [35], *SNTA1* [36] and *CACNA1C* [37]), giving strength to the possibility that these candidate genes also play a pathogenic role in LQTS. In particular, *RYR2* has previously been reported as gene associated with several arrhythmic diseases, including LQTS [38], catecholaminergic polymorphic ventricular tachycardia (CPVT) [39–41], arrhythmogenic right ventricular dysplasia type 2 [42–44] and sudden infant death syndrome [45]. Along with one candidate non-synonymous mutation (c.12892G>A [p.V4298M]) in *RYR2* that has been previously reported in LQTS [38], we identified nine additional candidate

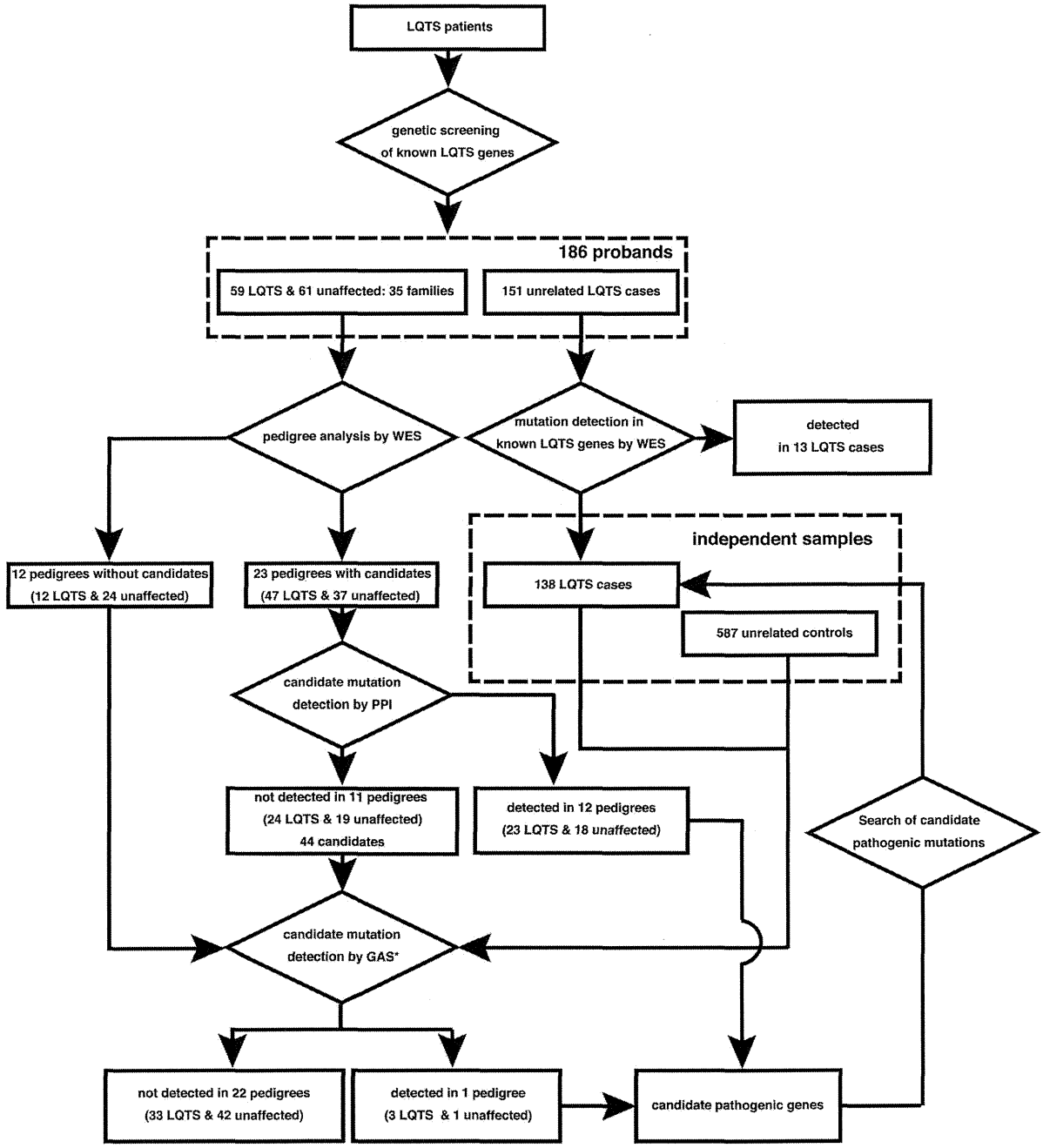

Fig 3. Experimental work flow for detecting candidate pathogenic mutations.

doi:10.1371/journal.pone.0130329.g003

Table 4. Significant association of *SLC2A5* detected by gene-based association study.

			Case			Control			
Transcript ID	cDNA level change	Protein level change	11	12	22	11	12	22	q-value
NM_003039.2	c.888C>G	p.I296M	0	4	157	0	1	585	0.014
	c.808C>T	p.R270W	0	1	160	0	0	587	
	c.457C>G	p.L153V	0	1	159	0	1	586	

doi:10.1371/journal.pone.0130329.t004

mutations (Table 6), strengthening the importance of *RYR2* in LQTS pathogenesis. PPI network analysis also revealed candidate pathogenic genes that interact directly or indirectly with known LQTS genes (*RIMS1* [46], *CIT* [47], *PIK3CG* [48], *SIRT6* [49] and *WDR26* [33]), implying that these candidate genes might also cause LQTS. In particular, *RIMS1* has been reported to regulate insulin secretory machinery [50]. Since insulin infusion has been shown to cause QTc prolongation in animal models [51, 52], this gene may be more likely to play a pathogenic role in LQTS.

A candidate gene based association study also identified an additional candidate pathogenic gene, *SLC2A5*, encoding a facilitated glucose/fructose transporter that plays a fundamental role in the pathogenesis of fructose-induced hypertension [53]. Since the mechanistic link between hypertension and fatal arrhythmia is not well-characterized, the role of this gene in the pathogenesis of long QT syndrome requires further investigation.

We examined the presence of mutations in the 11 candidate pathogenic genes in the genetically independent individuals. Most of the mutations were observed in calmodulin-interacting genes or known LQTS interacting genes (15 out of 16, Table 5), and many of these occurred at evolutionarily conserved amino acid across multiple species (10 out of 15). Since amino acid

Table 5. Candidate mutations in independent unrelated cases.

Gene	Transcript ID	cDNA level change	Protein level change	SIFT /PolyPhen-2*	Evolutionally conserved amino acid†
RYR2	NM_001035.2	c.497C>G	p.S166C	D/D	Conserved
RYR2	NM_001035.2	c.1259G>A	p.R420Q	D/D	
RYR2	NM_001035.2	c.1298T>C	p.L433P	D/B	Conserved
RYR2	NM_001035.2	c.5278C>T	p.R1760W	D/D	
RYR2	NM_001035.2	c.8470C>T	p.R2824W	D/D	
RYR2	NM_001035.2	c.11017C>T	p.R3673W	D/D	
RYR2	NM_001035.2	c.12438G>C	p.E4146D	D/D	Conserved
RYR2	NM_001035.2	c.13780A>C	p.K4594Q	D/D	Conserved
UBR4	NM_020765.2	c.1097A>G	p.K366R	T/P	Conserved
UBR4	NM_020765.2	c.1349G>T	p.R450L	D/D	Conserved
UBR4	NM_020765.2	c.1557G>C	p.Q519H	D/D	Conserved
UBR5	NM_015902.5	c.2965C>T	p.R989W	-/-	
PI4KA	NM_058004.2	c.738C>G	p.I246M	T/P	Conserved
KIF21B	NM_017596.2	c.2224G>A	p.E742K	D/P	Conserved
CIT	NM_001206999.1	c.5783C>T	p.A1928V	-/-	Conserved
WDR26	NM_001115113.2	c.59G>A	p.G20E	T/-	

*D = damaging; P = probably damaging; T = tolerated; B = benign.

†Conserved: evolutionally conserved amino acid in seven organisms: *Homo sapiens, Macaca mulatta, Mus musculus, Canis familiaris, Gallus gallus, Xenopus tropicalis and Danio rerio*.

Only candidate mutations in *WDR26* (c.59G>A [p.G20E]) and *RYR2* (c.11017C>T [p.R3673W]) were identified in the same individual.

doi:10.1371/journal.pone.0130329.t005

Table 6. Clinical background of patients with long-QT interval and *RYR2* mutation

cDNA level change	Protein level change	age	sex	Affected family members	QTc	event
c.497C>G	p.S166C	11	F	none	416	Syncope during swim, novel
c.1259G>A	p.R420Q	14	M	none	412	Syncope during swim (12 y), SD (17 y)
c.1298T>C	p.L433P	18	F	none	452	VF during exercise (17 y)
c.5278C>T	p.R1760W	16	M	none	425	Syncope during swim, novel
c.8470C>T	p.R2824W	7	M	none	439	Asympt, novel
c.11017C>T	p.R3673W	16	M	none	469	Heart failure, novel
c.12272C>T	p.A4091V	16	M	none	443	CA during exercise
c.12438G>C	p.E4146D	2	F	none	401	VF, novel
c.13780A>C	p.K4594Q	12	F	none	496	Syncope during swim (10 y), novel

doi:10.1371/journal.pone.0130329.t006

substitutions at evolutionarily conserved positions could potentially lead to deleterious effects on gene functions, these mutations may play an important role in the pathogenesis of LQTS.

To our knowledge, this study is the largest whole-exome sequencing analyses for LQTS. Our analysis revealed several novel candidate pathogenic genes through PPI analysis and gene-based association study. We believe our findings will be an anchor point for finding novel pathogenesis of this disorder.

Supporting Information

S1 Fig. Pedigree data. Samples with an asterisk were subject to WES analysis and those with a question mark have unknown affected status.
(PDF)

S2 Fig. Relatedness among Japanese, Han Chinese, European and African individuals. Plot of the first and the second principle components of the 749 subjects along with 45 East Asian (HapMap populations of Japanese in Tokyo: JPT), 45 Han Chinese in Beijing: CHB), 90 African (HapMap population of Yoruba in Ibadan, Nigeria: YRI), and 90 European (HapMap population of Utah, USA residents with ancestry from northern and western Europe: CEU) populations. The one outlier indicated by the arrow (case) was excluded.
(PDF)

S3 Fig. A quantile-quantile (QQ) plot for association results. The genomic inflation factor λ_{GC} was 1.027.
(TIFF)

S4 Fig. Coverage plots of all 120 individuals. Each line corresponds to one of the 120 individuals. On average, 92.8% of all target exons had at least 10-fold coverage.
(PDF)

S5 Fig. Missense mutations observed at evolutionally conserved amino acids across seven species. Homologous sequences were aligned using CLUSTALW. We identified evolutionally conserved amino acid across seven organisms: *Homo sapiens*, *Macaca mulatta*, *Mus musculus*, *Canis familiaris*, *Gallus gallus*, *Xenopus tropicalis* and *Danio rerio*.
(PDF)

S1 Table. Overview of exome-sequencing performance. † Proband.
(DOCX)

S2 Table. Variants detected in each of the 35 probands. † NS: non-synonymous SNV, SP: splice-site SNV. * Confirmed candidates: candidates co-segregated in the pedigree and validated using Sanger sequencing.
(DOCX)

S3 Table. Potential pathogenic mutations detected in 23 of the 35 families. † AR: autosomal recessive (HMZ = homozygous, CHTZ = compound heterozygous), AD: autosomal dominant. Bold: LQTS-susceptibility genes.
(DOCX)

Acknowledgments

We thank Keith A Boroevich for critical reading of our manuscript. We also thank the technical staff of the Laboratories for Medical Science Mathematics, Genome Sequencing Analysis and Cardiovascular Diseases at the RIKEN Center for Integrative Medical Sciences for the technical assistance.

Author Contributions

Performed the experiments: HN YS KO. Analyzed the data: DS TA. Contributed reagents/materials/analysis tools: AF FM. Wrote the paper: DS TA W. Shimizu T. Tanaka. Collected the samples: TA YM W. Satake T. Toda W. Shimizu T. Tanaka. Designed the study: MK T. Tsunoda W. Shimizu T. Tanaka.

References

1. Morita H, Wu J, Zipes DP. The QT syndromes: long and short. Lancet. 2008; 372(9640):750–63. Epub 2008/09/02. doi: 10.1016/S0140-6736(08)61307-0 S0140-6736(08)61307-0 [pii]. PMID: 18761222.
2. Schwartz PJ, Stramba-Badiale M, Crotti L, Pedrazzini M, Besana A, Bosi G, et al. Prevalence of the congenital long-QT syndrome. Circulation. 2009; 120(18):1761–7. Epub 2009/10/21. doi: 10.1161/CIRCULATIONAHA.109.863209 CIRCULATIONAHA.109.863209 [pii]. PMID: 19841298; PubMed Central PMCID: PMC2784143.
3. Boczek NJ, Best JM, Tester DJ, Giudicessi JR, Middha S, Evans JM, et al. Exome Sequencing and Systems Biology Converge to Identify Novel Mutations in the L-Type Calcium Channel, CACNA1C, Linked to Autosomal Dominant Long QT Syndrome. Circulation Cardiovascular genetics. 2013. Epub 2013/05/17. doi: CIRCGENETICS.113.000138 [pii]. doi: 10.1161/CIRCGENETICS.113.000138 PMID: 23677916.
4. Kiezun A, Garimella K, Do R, Stitziel NO, Neale BM, McLaren PJ, et al. Exome sequencing and the genetic basis of complex traits. Nature genetics. 2012; 44(6):623–30. Epub 2012/05/30. doi: 10.1038/ng.2303 ng.2303 [pii]. PMID: 22641211.
5. Choi M, Scholl UI, Ji W, Liu T, Tikhonova IR, Zumbo P, et al. Genetic diagnosis by whole exome capture and massively parallel DNA sequencing. Proc Natl Acad Sci U S A. 2009; 106(45):19096–101. Epub 2009/10/29. doi: 10.1073/pnas.0910672106 0910672106 [pii]. PMID: 19861545; PubMed Central PMCID: PMC2768590.
6. Ng SB, Buckingham KJ, Lee C, Bigham AW, Tabor HK, Dent KM, et al. Exome sequencing identifies the cause of a mendelian disorder. Nature genetics. 2010; 42(1):30–5. Epub 2009/11/17. doi: 10.1038/ng.499 ng.499 [pii]. PMID: 19915526; PubMed Central PMCID: PMC2847889.
7. Wei X, Walia V, Lin JC, Teer JK, Prickett TD, Gartner J, et al. Exome sequencing identifies GRIN2A as frequently mutated in melanoma. Nature genetics. 2011; 43(5):442–6. Epub 2011/04/19. doi: 10.1038/ng.810 ng.810 [pii]. PMID: 21499247; PubMed Central PMCID: PMC3161250.
8. Varela I, Tarpey P, Raine K, Huang D, Ong CK, Stephens P, et al. Exome sequencing identifies frequent mutation of the SWI/SNF complex gene PBRM1 in renal carcinoma. Nature. 2011; 469(7331):539–42. Epub 2011/01/21. doi: 10.1038/nature09639 nature09639 [pii]. PMID: 21248752; PubMed Central PMCID: PMC3030920.
9. Agrawal N, Frederick MJ, Pickering CR, Bettegowda C, Chang K, Li RJ, et al. Exome sequencing of head and neck squamous cell carcinoma reveals inactivating mutations in NOTCH1. Science. 2011;

333(6046):1154–7. Epub 2011/07/30. doi: 10.1126/science.1206923 science.1206923 [pii]. PMID: 21798897; PubMed Central PMCID: PMC3162986.

10. Schwartz PJ, Crotti L. QTc behavior during exercise and genetic testing for the long-QT syndrome. Circulation. 2011; 124(20):2181–4. doi: 10.1161/CIRCULATIONAHA.111.062182 PMID: 22083145.
11. Wang Q, Curran ME, Splawski I, Burn TC, Millholland JM, VanRaay TJ, et al. Positional cloning of a novel potassium channel gene: KVLQT1 mutations cause cardiac arrhythmias. Nature genetics. 1996; 12(1):17–23. doi: 10.1038/ng0196-17 PMID: 8528244.
12. Napolitano C, Priori SG, Schwartz PJ, Bloise R, Ronchetti E, Nastoli J, et al. Genetic testing in the long QT syndrome: development and validation of an efficient approach to genotyping in clinical practice. Jama. 2005; 294(23):2975–80. doi: 10.1001/jama.294.23.2975 PMID: 16414944.
13. Itoh H, Shimizu W, Hayashi K, Yamagata K, Sakaguchi T, Ohno S, et al. Long QT syndrome with compound mutations is associated with a more severe phenotype: a Japanese multicenter study. Heart rhythm: the official journal of the Heart Rhythm Society. 2010; 7(10):1411–8. doi: 10.1016/j.hrthm.2010.06.013 PMID: 20541041.
14. Nishio Y, Makiyama T, Itoh H, Sakaguchi T, Ohno S, Gong YZ, et al. D85N, a KCNE1 polymorphism, is a disease-causing gene variant in long QT syndrome. Journal of the American College of Cardiology. 2009; 54(9):812–9. doi: 10.1016/j.jacc.2009.06.005 PMID: 19695459.
15. Li H, Durbin R. Fast and accurate short read alignment with Burrows-Wheeler transform. Bioinformatics. 2009; 25(14):1754–60. Epub 2009/05/20. doi: 10.1093/bioinformatics/btp324 btp324 [pii]. PMID: 19451168; PubMed Central PMCID: PMC2705234.
16. Li H, Handsaker B, Wysoker A, Fennell T, Ruan J, Homer N, et al. The Sequence Alignment/Map format and SAMtools. Bioinformatics. 2009; 25(16):2078–9. doi: 10.1093/bioinformatics/btp352 PMID: 19505943; PubMed Central PMCID: PMC2723002.
17. Shigemizu D, Fujimoto A, Akiyama S, Abe T, Nakano K, Boroevich KA, et al. A practical method to detect SNVs and indels from whole genome and exome sequencing data. Sci Rep. 2013; 3:2161. Epub 2013/07/09. doi: 10.1038/srep02161 srep02161 [pii]. PMID: 23831772; PubMed Central PMCID: PMC3703611.
18. McKenna A, Hanna M, Banks E, Sivachenko A, Cibulskis K, Kernytsky A, et al. The Genome Analysis Toolkit: a MapReduce framework for analyzing next-generation DNA sequencing data. Genome Res. 2010; 20(9):1297–303. Epub 2010/07/21. doi: 10.1101/gr.107524.110 gr.107524.110 [pii]. PMID: 20644199; PubMed Central PMCID: PMC2928508.
19. Smigielski EM, Sirotkin K, Ward M, Sherry ST. dbSNP: a database of single nucleotide polymorphisms. Nucleic Acids Res. 2000; 28(1):352–5. Epub 1999/12/11. doi: gkd114 [pii]. PMID: 10592272; PubMed Central PMCID: PMC102496.
20. Via M, Gignoux C, Burchard EG. The 1000 Genomes Project: new opportunities for research and social challenges. Genome Med. 2010; 2(1):3. Epub 2010/03/03. doi: 10.1186/gm124 gm124 [pii]. PMID: 20193048; PubMed Central PMCID: PMC2829928.
21. Fu W, O'Connor TD, Jun G, Kang HM, Abecasis G, Leal SM, et al. Analysis of 6,515 exomes reveals the recent origin of most human protein-coding variants. Nature. 2013; 493(7431):216–20. Epub 2012/12/04. doi: 10.1038/nature11690 nature11690 [pii]. PMID: 23201682; PubMed Central PMCID: PMC3676746.
22. Kumar P, Henikoff S, Ng PC. Predicting the effects of coding non-synonymous variants on protein function using the SIFT algorithm. Nat Protoc. 2009; 4(7):1073–81. Epub 2009/06/30. doi: 10.1038/nprot.2009.86 nprot.2009.86 [pii]. PMID: 19561590.
23. Adzhubei IA, Schmidt S, Peshkin L, Ramensky VE, Gerasimova A, Bork P, et al. A method and server for predicting damaging missense mutations. Nat Methods. 2010; 7(4):248–9. Epub 2010/04/01. doi: 10.1038/nmeth0410-248 nmeth0410-248 [pii]. PMID: 20354512; PubMed Central PMCID: PMC2855889.
24. Novembre J, Stephens M. Interpreting principal component analyses of spatial population genetic variation. Nature genetics. 2008; 40(5):646–9. doi: 10.1038/ng.139 PMID: 18425127; PubMed Central PMCID: PMC3989108.
25. Purcell S, Neale B, Todd-Brown K, Thomas L, Ferreira MA, Bender D, et al. PLINK: a tool set for whole-genome association and population-based linkage analyses. Am J Hum Genet. 2007; 81(3):559–75. doi: 10.1086/519795 PMID: 17701901; PubMed Central PMCID: PMC1950838.
26. Team RDC. R: A Language and Environment for Statistical Computing. Vienna, Austria: R Foundation for Statistical Computing. 2009.
27. Lee S, Wu MC, Lin X. Optimal tests for rare variant effects in sequencing association studies. Biostatistics. 2012; 13(4):762–75. doi: 10.1093/biostatistics/kxs014 PMID: 22699862; PubMed Central PMCID: PMC3440237.

28. Li B, Leal SM. Methods for detecting associations with rare variants for common diseases: application to analysis of sequence data. Am J Hum Genet. 2008; 83(3):311–21. doi: 10.1016/j.ajhg.2008.06.024 PMID: 18691683; PubMed Central PMCID: PMC2842185.

29. Wu MC, Lee S, Cai T, Li Y, Boehnke M, Lin X. Rare-variant association testing for sequencing data with the sequence kernel association test. Am J Hum Genet. 2011; 89(1):82–93. doi: 10.1016/j.ajhg.2011.05.029 PMID: 21737059; PubMed Central PMCID: PMC3135811.

30. Makita N, Yagihara N, Crotti L, Johnson CN, Beckmann BM, Roh MS, et al. Novel calmodulin mutations associated with congenital arrhythmia susceptibility. Circulation Cardiovascular genetics. 2014; 7(4):466–74. doi: 10.1161/CIRCGENETICS.113.000459 PMID: 24917665; PubMed Central PMCID: PMC4140998.

31. Hino A, Yano M, Kato T, Fukuda M, Suetomi T, Ono M, et al. Enhanced binding of calmodulin to the ryanodine receptor corrects contractile dysfunction in failing hearts. Cardiovasc Res. 2012; 96(3):433–43. Epub 2012/08/16. doi: 10.1093/cvr/cvs271 cvs271 [pii]. PMID: 22893680; PubMed Central PMCID: PMC3584972.

32. Nakatani Y, Konishi H, Vassilev A, Kurooka H, Ishiguro K, Sawada J, et al. p600, a unique protein required for membrane morphogenesis and cell survival. Proc Natl Acad Sci U S A. 2005; 102(42):15093–8. Epub 2005/10/11. 0507458102 [pii]. doi: 10.1073/pnas.0507458102 PMID: 16214886; PubMed Central PMCID: PMC1247991.

33. Alexandru G, Graumann J, Smith GT, Kolawa NJ, Fang R, Deshaies RJ. UBXD7 binds multiple ubiquitin ligases and implicates p97 in HIF1alpha turnover. Cell. 2008; 134(5):804–16. Epub 2008/09/09. doi: 10.1016/j.cell.2008.06.048 S0092-8674(08)00835-0 [pii]. PMID: 18775313; PubMed Central PMCID: PMC2614663.

34. Berggard T, Arrigoni G, Olsson O, Fex M, Linse S, James P. 140 mouse brain proteins identified by Ca2+-calmodulin affinity chromatography and tandem mass spectrometry. J Proteome Res. 2006; 5(3):669–87. doi: 10.1021/pr050421l PMID: 16512683.

35. Tan HL, Kupershmidt S, Zhang R, Stepanovic S, Roden DM, Wilde AA, et al. A calcium sensor in the sodium channel modulates cardiac excitability. Nature. 2002; 415(6870):442–7. Epub 2002/01/25. doi: 10.1038/415442a 415442a [pii]. PMID: 11807557.

36. Iwata Y, Pan Y, Yoshida T, Hanada H, Shigekawa M. Alpha1-syntrophin has distinct binding sites for actin and calmodulin. FEBS Lett. 1998; 423(2):173–7. Epub 1998/03/25. doi: S0014-5793(98)00085-4 [pii]. PMID: 9512352.

37. Xiong L, Kleerekoper QK, He R, Putkey JA, Hamilton SL. Sites on calmodulin that interact with the C-terminal tail of Cav1.2 channel. J Biol Chem. 2005; 280(8):7070–9. Epub 2004/12/08. doi: M410558200 [pii]. doi: 10.1074/jbc.M410558200 PMID: 15583004.

38. Kauferstein S, Kiehne N, Erkapic D, Schmidt J, Hamm CW, Bratzke H, et al. A novel mutation in the cardiac ryanodine receptor gene (RyR2) in a patient with an unequivocal LQTS. Int J Cardiol. 2011; 146(2):249–50. Epub 2010/12/04. doi: 10.1016/j.ijcard.2010.10.062 S0167-5273(10)00910-1 [pii]. PMID: 21126784.

39. Hayashi M, Denjoy I, Extramiana F, Maltret A, Buisson NR, Lupoglazoff JM, et al. Incidence and risk factors of arrhythmic events in catecholaminergic polymorphic ventricular tachycardia. Circulation. 2009; 119(18):2426–34. Epub 2009/04/29. doi: 10.1161/CIRCULATIONAHA.108.829267 CIRCULATIONAHA.108.829267 [pii]. PMID: 19398665.

40. Jiang D, Jones PP, Davis DR, Gow R, Green MS, Birnie DH, et al. Characterization of a novel mutation in the cardiac ryanodine receptor that results in catecholaminergic polymorphic ventricular tachycardia. Channels (Austin). 2010; 4(4):302–10. Epub 2010/08/03. doi: 12666 [pii]. PMID: 20676041; PubMed Central PMCID: PMC3322479.

41. Meli AC, Refaat MM, Dura M, Reiken S, Wronska A, Wojciak J, et al. A novel ryanodine receptor mutation linked to sudden death increases sensitivity to cytosolic calcium. Circ Res. 2011; 109(3):281–90. Epub 2011/06/11. doi: 10.1161/CIRCRESAHA.111.244970 CIRCRESAHA.111.244970 [pii]. PMID: 21659649; PubMed Central PMCID: PMC3690513.

42. Tiso N, Stephan DA, Nava A, Bagattin A, Devaney JM, Stanchi F, et al. Identification of mutations in the cardiac ryanodine receptor gene in families affected with arrhythmogenic right ventricular cardiomyopathy type 2 (ARVD2). Hum Mol Genet. 2001; 10(3):189–94. Epub 2001/02/13. PMID: 11159936.

43. Jiang D, Wang R, Xiao B, Kong H, Hunt DJ, Choi P, et al. Enhanced store overload-induced Ca2+ release and channel sensitivity to luminal Ca2+ activation are common defects of RyR2 mutations linked to ventricular tachycardia and sudden death. Circ Res. 2005; 97(11):1173–81. Epub 2005/10/22. doi: 01.RES.0000192146.85173.4b [pii]. doi: 10.1161/01.RES.0000192146.85173.4b PMID: 16239587.

44. Tang Y, Tian X, Wang R, Fill M, Chen SR. Abnormal termination of Ca2+ release is a common defect of RyR2 mutations associated with cardiomyopathies. Circ Res. 2012; 110(7):968–77. Epub 2012/03/01.

doi: 10.1161/CIRCRESAHA.111.256560 CIRCRESAHA.111.256560 [pii]. PMID: 22374134; PubMed Central PMCID: PMC3345272.

45. Tester DJ, Dura M, Carturan E, Reiken S, Wronska A, Marks AR, et al. A mechanism for sudden infant death syndrome (SIDS): stress-induced leak via ryanodine receptors. Heart rhythm: the official journal of the Heart Rhythm Society. 2007; 4(6):733–9. Epub 2007/06/09. doi: S1547-5271(07)00227-5 [pii]. doi: 10.1016/j.hrthm.2007.02.026 PMID: 17556193; PubMed Central PMCID: PMC3332548.

46. Coppola T, Magnin-Luthi S, Perret-Menoud V, Gattesco S, Schiavo G, Regazzi R. Direct interaction of the Rab3 effector RIM with Ca2+ channels, SNAP-25, and synaptotagmin. J Biol Chem. 2001; 276 (35):32756–62. doi: 10.1074/jbc.M100929200 PMID: 11438518.

47. Carter CJ. eIF2B and oligodendrocyte survival: where nature and nurture meet in bipolar disorder and schizophrenia? Schizophr Bull. 2007; 33(6):1343–53. doi: 10.1093/schbul/sbm007 PMID: 17329232; PubMed Central PMCID: PMC2779884.

48. Viard P, Butcher AJ, Halet G, Davies A, Nurnberg B, Heblich F, et al. PI3K promotes voltage-dependent calcium channel trafficking to the plasma membrane. Nature neuroscience. 2004; 7(9):939–46. doi: 10. 1038/nn1300 PMID: 15311280.

49. Sundaresan NR, Vasudevan P, Zhong L, Kim G, Samant S, Parekh V, et al. The sirtuin SIRT6 blocks IGF-Akt signaling and development of cardiac hypertrophy by targeting c-Jun. Nature medicine. 2012; 18(11):1643–50. doi: 10.1038/nm.2961 PMID: 23086477.

50. Gandini MA, Sandoval A, Gonzalez-Ramirez R, Mori Y, de Waard M, Felix R. Functional coupling of Rab3-interacting molecule 1 (RIM1) and L-type Ca2+ channels in insulin release. J Biol Chem. 2011; 286(18):15757–65. doi: 10.1074/jbc.M110.187757 PMID: 21402706; PubMed Central PMCID: PMC3091184.

51. van Noord C, Sturkenboom MC, Straus SM, Hofman A, Kors JA, Witteman JC, et al. Serum glucose and insulin are associated with QTc and RR intervals in nondiabetic elderly. Eur J Endocrinol. 2010; 162(2):241–8. doi: 10.1530/EJE-09-0878 PMID: 19897609.

52. Drimba L, Dobronte R, Hegedus C, Sari R, Di Y, Nemeth J, et al. The role of acute hyperinsulinemia in the development of cardiac arrhythmias. Naunyn Schmiedebergs Arch Pharmacol. 2013; 386(5):435–44. doi: 10.1007/s00210-013-0845-4 PMID: 23474828.

53. Barone S, Fussell SL, Singh AK, Lucas F, Xu J, Kim C, et al. Slc2a5 (Glut5) is essential for the absorption of fructose in the intestine and generation of fructose-induced hypertension. J Biol Chem. 2009; 284(8):5056–66. doi: 10.1074/jbc.M808128200 PMID: 19091748; PubMed Central PMCID: PMC2643499.

Original Article

Functional Characterization of Rare Variants Implicated in Susceptibility to Lone Atrial Fibrillation

Kenshi Hayashi, MD, PhD; Tetsuo Konno, MD, PhD; Hayato Tada, MD, PhD; Satoyuki Tani, BS; Li Liu, MD, PhD; Noboru Fujino, MD, PhD; Atsushi Nohara, MD, PhD; Akihiko Hodatsu, MD, PhD; Toyonobu Tsuda, MD; Yoshihiro Tanaka, MD; Masa-aki Kawashiri, MD, PhD; Hidekazu Ino, MD, PhD; Naomasa Makita, MD, PhD; Masakazu Yamagishi, MD, PhD

Background—Few rare variants in atrial fibrillation (AF)–associated genes have been functionally characterized to identify a causal relationship between these variants and development of AF. We here sought to determine the clinical effect of rare variants in AF-associated genes in patients with lone AF and characterized these variants electrophysiologically and bioinformatically.

Methods and Results—We screened all coding regions in 12 AF-associated genes in 90 patients with lone AF, with an onset of 47±11 years (66 men; mean age, 56±13 years) by high-resolution melting curve analysis and DNA sequencing. The potassium and sodium currents were analyzed using whole-cell patch clamping. In addition to using 4 individual in silico prediction tools, we extended those predictions to an integrated tool (Combined Annotation Dependent Depletion). We identified 7 rare variants in *KCNA5*, *KCNQ1*, *KCNH2*, *SCN5A*, and *SCN1B* genes in 8 patients: 2 of 8 probands had a family history of AF. Electrophysiological studies revealed that 2 variants showed a loss-of-function, and 4 variants showed a gain-of-function. Five of 6 variants with electrophysiological abnormalities were predicted as pathogenic by Combined Annotation Dependent Depletion scores.

Conclusions—In our cohort of patients with lone AF, 7 rare variants in cardiac ion channels were identified in 8 probands. A combination of electrophysiological studies and in silico predictions showed that these variants could contribute to the development of lone AF, although further in vivo study is necessary to confirm these results. More than half of AF-associated rare variants showed gain-of-function behavior, which may be targeted using genotype-specific pharmacological therapy. (***Circ Arrhythm Electrophysiol.* 2015;8:1095-1104. DOI: 10.1161/CIRCEP.114.002519.**)

Key Words: analysis of variance ■ atrial fibrillation ■ genetic association studies ■ genetic variation ■ ion channels

Atrial fibrillation (AF) is the most prevalent tachyarrhythmia, with a prevalence of 1% to 2% in the general population.[1] In most cases, AF occurs along with hypertension, mitral stenosis, ischemic heart disease, cardiomyopathy, and hyperthyroidism.[1] In addition to these underlying diseases, age, obesity, smoking, and alcohol are clinical risk factors for AF.[1] However, 11% of AF patients present with AF in the absence of predisposing factors; these are categorized as having lone AF.[2] Previous studies have shown that at least 5% of all patients with AF and 15% of those with lone AF had a positive family history.[3] Another study has shown that the risk for lone AF was 3.5× higher in those with a family history of lone AF in parents or in siblings, compared with the risk in individuals without such family history.[4] Recent studies have shown that people with certain genotypes have an increased risk for future AF.[5,6] These reports indicate that the development of AF is influenced by genetic background.

Editorial see p 1005

Genetic linkage analysis and candidate gene analysis for familial AF in 1997 indicated that a gene responsible for familial AF is located in the region of 10q22 to 10q24, and in 2003, a gain-of-function mutation in *KCNQ1* was implicated in a large Chinese kindred with autosomal dominant AF.[7] To date, many variants in genes encoding ion-channel subunits, cardiac gap junctions, and signaling molecules have been identified in monogenic AF families.[8,9] These genetic variants predispose individuals to AF by reducing the atrial refractory period as a substrate for re-entrant arrhythmias, by lengthening the atrial action potential duration, which results in ectopic activity, or by causing impaired

Received November 7, 2014; accepted June 19, 2015.

From the Division of Cardiovascular Medicine, Kanazawa University Graduate School of Medicine, Kanazawa, Japan (K.H., T.K., H.T., S.T., L.L., N.F., A.N., A.H., T.T., Y.T., M.K., M.Y.); Department of Cardiology, Komatsu Municipal Hospital, Komatsu, Japan (H.I.); and Department of Molecular Physiology, Nagasaki University Graduate School of Biomedical Sciences, Nagasaki, Japan (N.M.).

The Data Supplement is available at http://circep.ahajournals.org/lookup/suppl/doi:10.1161/CIRCEP.114.002519/-/DC1.

Correspondence to Kenshi Hayashi, MD, PhD, Division of Cardiovascular Medicine, Kanazawa University Graduate School of Medical Science, 13-1, Takara-machi, Kanazawa, Ishikawa 920-8640, Japan. E-mail kenshi@med.kanazawa-u.ac.jp

Circ Arrhythm Electrophysiol **is available at http://circep.ahajournals.org** **DOI: 10.1161/CIRCEP.114.002519**

WHAT IS KNOWN

- To date, many variants in genes encoding ion-channel subunits, cardiac gap junctions, and signaling molecules have been identified in monogenic families with atrial fibrillation (AF) and patients with lone AF.
- Few rare variants in AF-associated genes have been functionally characterized to identify a causal relationship between these variants and development of AF.

WHAT THE STUDY ADDS

- We identified 7 rare variants in cardiac ion channels in 8 probands from 90 patients with lone AF, indicating a prevalence of ≈9%.
- These variants were extremely rare and characterized as causing susceptibility to AF by either electrophysiological study or in silico prediction analysis including a new prediction tool, Combined Annotation Dependent Depletion scores.
- More than half of AF-associated rare variants showed gain-of-function behavior, which is likely to benefit from a drug that blocks particular ion channels.

electric cell-to-cell communication, which creates conduction heterogeneity as a substrate for the maintenance of AF.[10]

Here, we performed candidate gene studies to identify rare variants, under the hypothesis that these variants pose an AF risk in these probands. In addition, to determine the functional significance of these variants, we performed cellular electrophysiological studies and in silico prediction analysis.

Methods

Detailed description of Methods is provided in the Data Supplement.

Study Subjects

The study subjects were recruited from multiple hospitals in Japan. Lone AF was defined as AF occurring in individuals aged <65 years, who did not present with hypertension, overt structural heart disease, myocardial infarction, congestive heart failure, or thyroid dysfunction. Two hundred fifty healthy Japanese subjects with no history of the cardiovascular disease described above were also included in this study. Data from the National Heart, Lung, and Blood Institute Exome Sequencing Project Exome Variant Server (EVS)[11] and the Exome Aggregation Consortium (ExAC) data and browser[12] were used as reference groups.

The study observed the principles outlined in the Declaration of Helsinki and was approved by the Ethics Committee for Medical Research at our institution. All study patients provided written informed consent before registration.

DNA Isolation and Mutation Analysis and Genotype–Phenotype Relationships

Genomic DNA was extracted from peripheral blood leukocytes using standard methods. High-resolution melting curve analysis was used to screen *KCNA5*, *KCNQ1*, *KCNH2*, *SCN5A*, *SCN1B*, *SCN2B*, *SCN3B*, *KCNE1*, *KCNE2*, *KCNJ5*, *GJA5*, and *NPPA* using a LightScanner (BioFire Defense, Salt Lake City, UT). Samples in which the melting curve deviated from the wild-type (WT) control were subjected to DNA sequencing using an ABI PRISM 310 Genetic Analyzer. The relationship between the clinical phenotype (AF) and the genotype was determined for probands and their relatives in whom a variant was identified.

Plasmid Constructs and Electrophysiology

Mutant cDNAs were constructed using an overlap extension strategy[13] or by using the QuikChange XL Site-Directed Mutagenesis Kit (Agilent Technologies, Santa Clara, CA). CHO-K1 or HEK293 cells were transiently transfected with WT or mutant cDNA, using an X-tremeGENE 9 DNA Transfection Reagent (Roche Applied Science, Penzberg, Germany). Cells were cotransfected with the same amount of green fluorescent protein as each ion-channel cDNA.

Cells displaying green fluorescence at 48 to 72 hours after transfection were subjected to electrophysiological analysis. Potassium or sodium currents were studied using the whole-cell patch clamp technique with an amplifier, Axopatch-200B (Molecular Devices, Sunnyvale, CA), at room temperature. The voltage clamp protocols are described in the figures. Data were acquired using pCLAMP software (version 9; Molecular Devices, Sunnyvale, CA). Data acquisition and analysis were performed using a Digidata 1321 A/D converter and pCLAMP8.2 software (Molecular Devices, Sunnyvale, CA).

In Silico Prediction Analysis

A total of 5 prediction tools were applied to predict the pathogenicity of lone AF-associated variants: the PolyPhen algorithm,[14] Grantham chemical scores,[14] Sorting Intolerant From Tolerant analysis,[14] the Protein Variation Effect Analyzer,[15] and Combined Annotation Dependent Depletion (CADD).[16]

Statistical Analysis

Pooled electrophysiological data were expressed as mean±SE. The minor allele frequency (MAF) in the AF cohort was compared with the MAF from the EVS and the ExAC using Fisher exact test in 2×2 tables. Two-tailed Student *t* test was used for the single comparisons between the 2 groups. One-way ANOVA, followed by a Bonferroni post hoc test, was used to analyze data with unequal variance among 3 groups. Two-way repeated-measures ANOVA was used to adjust for multiple comparisons across the different values of membrane potentials. A value of $P<0.05$ was considered as statistically significant. Statistical analysis was performed using JMP Pro 11.0.0 (SAS Institute Inc, NC) and Origin 9.0 (OriginLab, Northampton, MA).

Results

Clinical Characteristics and Molecular Genetic Analysis of the Study Cohort

Of the 90 patients with lone AF that were enrolled, 26 subjects (29%) had a family history of AF in at least 1 first-degree relative (Table 1). The study subjects had a mean age of 47±11 years at the onset of AF (Table 1). Sixty-six subjects were men (73%), and 57 of the 90 patients had paroxysmal or persistent AF (63%; Table 1). Echocardiographic data of the cohort as a whole revealed a normal mean ejection fraction, with a mean left atrial dimension of 40±7 mm (Table 1). The 250 control subjects had a mean age of 39±19 years, and 157 of them were men (63%).

Screening for ion-channel variants in genomic DNA in the study cohort of 90 individuals with lone AF identified a total of 7 different variants present in *KCNA5* (H463R and T527M), *KCNQ1* (L492_E493 ins DL), *KCNH2* (T436M and T895M), *SCN5A* (R986Q), and *SCN1B* (T189M; Figure 1; Table 2). *SCN1B* T189M was detected in 2 probands (1 homozygous and 1

Table 1. Clinical Characteristics of the Lone AF Population

Total	90
Age at onset AF, y	47±11
Age at enrollment, y	56±13
Male sex (%)	66 (73)
Family history (%)	26 (29)
AF type	
Paroxysmal or persistent (%)	57 (63)
Permanent (%)	33 (37)
Complication	
Bradyarrhythmia (%)	10 (11)
Brugada syndrome (%)	3 (3)
Echocardiogram	
Left atrial size, mm	40±7
Ejection fraction (%)	65±8
Catheter ablation (%)	20 (22)

AF indicates atrial fibrillation.

heterozygous carrier). The presence of each of these variants was assessed in 250 ethnically matched population control individuals; all variants were rare (MAF, <1%; Table 2). According to the ExAC data and browser, the MAFs of *KCNA5* T527M, *KCNH2* T436M, and *SCN5A* R986Q were 0.0236%, 0.001627%, and 0.001951%, respectively, which were significantly lower compared with 0.6% in our case population (Table 2).

Clinical Characteristics and Functional Properties of *KCNA5* Variants

The proband who was heterozygous for *KCNA5* H463R was a 62-year-old woman with onset of paroxysmal AF at the age of 51 and no family history of AF. She underwent radiofrequency catheter ablation at the age of 61 (Table 3).

To define the functional effect of the H463R variant, we transiently expressed WT, H463R, and WT+H463R in cultured mammalian HEK293 cells for whole-cell voltage clamp measurements. Voltage clamp recording from cells expressing H463R alone did not exhibit any functional channels, when compared with those expressing WT alone (Figure 2A; Table 4). Coexpression of H463R with WT resulted in a significant current density, which was less than one-third of the control current observed with the expression of WT alone (Figure 2A).

The current–voltage relationships for activating currents (Figure 2B) and tail currents (Figure 2C) were recorded during depolarizing pulses. Two-way repeated-measures ANOVA revealed that there was a significant difference in the activating currents and the tail currents (Figure 2B and 2C) among these 3 channels. The amplitudes of the activating currents at 40 mV and the tail currents at 30 mV for the WT+H463R and the H463R were significantly smaller than those for WT (Figure 2B and 2C; Table I in the Data Supplement). No significant difference in activation kinetics for the WT+H463R was observed compared with WT (Figure 2D; Table I in the Data Supplement). In silico analysis predicted that H463R was pathogenic, according to 3 algorithms (Table 5).

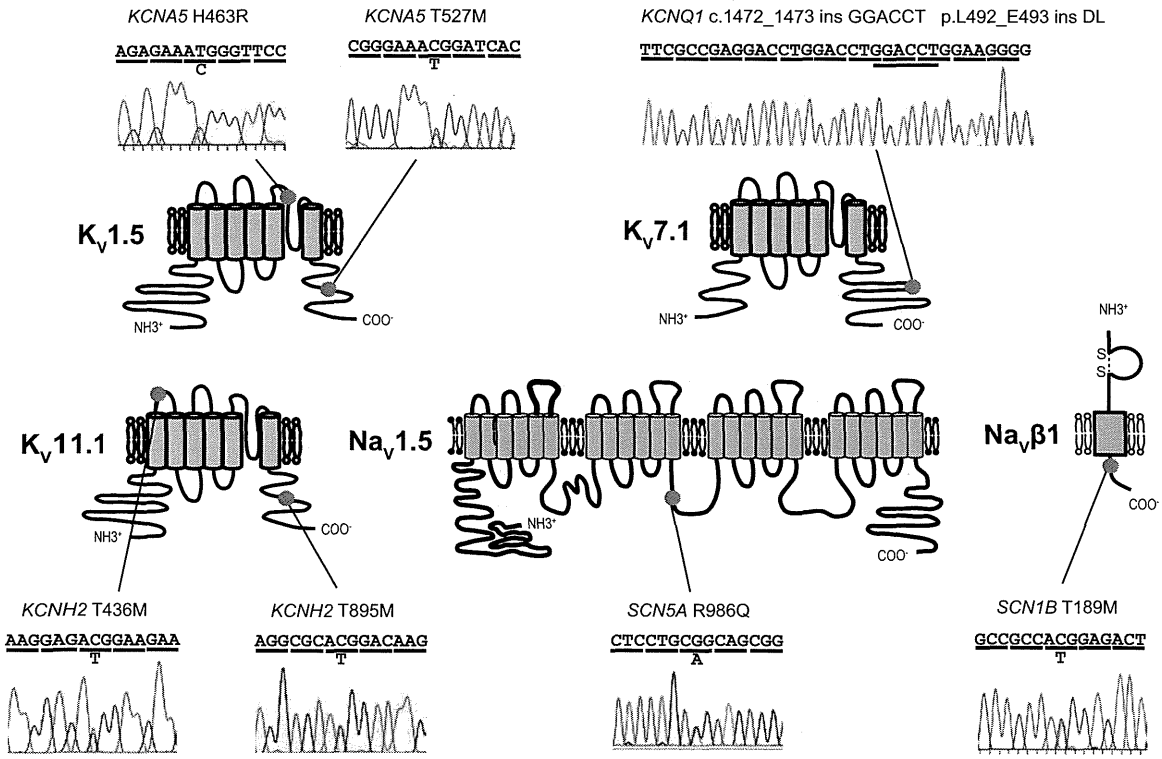

Figure 1. Sequencing of *KCNA5*, *KCNQ1*, *KCNH2*, *SCN5A*, and *SCN1B*. DNA sequencing electropherograms demonstrated 7 genetic variants. The KCNQ1 insertion variant was confirmed by sequencing the mutant allele in *KCNQ1*. The topology of the voltage-gated ion channels shows the location of the detected variants.

Table 2. Summary of Ion-Channel Rare Variants

		AF Probands, n=90			Controls, n=250			Exome Variant Server			Exome Aggregation Consortium		
Gene	Amino Acid Change	Allele Count	Allele Number	MAF	Allele Count	Allele Number	MAF	Allele Count	Allele Number	MAF	Allele count	Allele number	MAF
KCNA5	H463R	1	180	0.006	0	500	0	N/A	N/A	N/A	N/A	N/A	N/A
	T527M	1	180	0.006	1	500	0.002	N/A	N/A	N/A	29	122816	0.000236†
KCNQ1	L492_E493 ins DL	1	180	0.006	0	500	0	N/A	N/A	N/A	N/A	N/A	N/A
KCNH2	T436M	1	180	0.006	0	500	0	N/A	N/A	N/A	2	122940	1.627×10^{-5}*
	T895M	1	180	0.006	0	500	0	N/A	N/A	N/A	N/A	N/A	N/A
SCN5A	R986Q	1	180	0.006	0	500	0	1	12116	8.253×10^{-5}†	2	102516	1.951×10^{-5}*
SCN1B	T189M	3	180	0.017	1	500	0.002	N/A	N/A	N/A	N/A	N/A	N/A

AF indicates atrial fibrillation; MAF, minor allele frequency; and N/A, not available.
*$P<0.01$ vs MAF of probands.
†$P<0.05$ vs MAF of AF probands.

The proband who was heterozygous for *KCNA5* T527M was a 51-year-old man, with onset of paroxysmal AF at the age of 49 (Table 3). The ECG showed a prolonged PR interval of 220 ms and a normal QTc interval. Monitoring ECG in an outpatient clinic showed a sinus pause of 3.6 s after termination of AF. His son, who also carried the T527M variant in *KCNA5*, had never experienced AF and had a prolonged PR interval of 220 ms.

HEK293 cells expressing the T527M mutant showed a larger Kv1.5 current than did those expressing WT (Figure 3A). Cellular electrophysiological studies showed that the activating current density for T527M was significantly larger than that for WT (Figure 3B; Table I in the Data Supplement; Table 4). The T527M mutant displayed a negative voltage shift in the normalized activation curve and a significantly decreased the potential when half of the channels were activated, $V_{1/2}$ (Figure 3D; Table I in the Data Supplement). In silico analysis using 4 algorithms predicted that T527M was pathogenic (Table 5).

Clinical Characteristics and Functional Properties of *KCNQ1* Variants

The proband who was heterozygous for *KCNQ1* L492_E493insDL was a 42-year-old man who was diagnosed with AF on an ECG on routine examination (Table 3). Because he had no symptoms, the age of onset of paroxysmal AF was unknown. The ECG showed a normal QTc interval at rest and during the late recovery phase of exercise stress testing. His daughter and sons carrying the L492_E493insDL variant in *KCNQ1* had never experienced AF and had normal ECGs.

Table 3. Clinical Characteristics of Patients With Rare Variants

Proband Number	Patient Type	Age, y	Genotype	Sex	Family History	Phenotype	Onset, y	ECG, HR/ PR/QRS/QTc	Echocardiography LAD (mm)/EF (%)	Catheter Ablation
1	Proband	62	*KCNA5* H463R	F	No	Persistent	51	67/0.14/0.08/0.452	34/66	Yes
2	Proband	51	*KCNA5* T527M	M	No	Persistent	49	67/0.22/0.07/0.391	35/70	No
	Son	29	*KCNA5* T527M	M	No	AF(−)		77/0.22/0.10/0.395	...	No
3	Proband	42	*KCNQ1* L492_E493 ins DL	M	No	Paroxysmal	42	68/0.19/0.08/0.392	36/53	No
	Daughter	18	*KCNQ1* L492_E493 ins DL	F	No	AF(−)	...	58/0.144/0.09/0.387	...	No
	Son	16	*KCNQ1* L492_E493 ins DL	M	No	AF(−)	...	54/0.16/0.09/0.426	...	No
	Son	7	*KCNQ1* L492_E493 ins DL	M	No	AF(−)	...	81/0.146/0.07/0.437	...	No
4	Proband	61	*KCNH2* T436M	M	Yes	Chronic	38	73/-/0.08/0.371	49/73	No
5	Proband	58	*KCNH2* T895M	M	Yes	Persistent	40	64/0.15/0.10/0.405	42/63	Yes
	Father	87	*KCNH2* T895M	M	Yes	Paroxysmal palpitation	50s	69/0.17/0.11/0.451	...	No
	Son	37	*KCNH2* T895M	M	Yes	Paroxysmal palpitation	20s	59/0.16/0.11/0.386	...	No
6	Proband	64	*SCN5A* R986Q	M	No	Paroxysmal	58	52/0.134/0.11/0.369	37/70	No
7	Proband	59	*SCN1B* T189M (homozygous)	F	No	Paroxysmal	59	50/0.151/0.09/0.378	30/76	No
	Daughter	33	*SCN1B* T189M (heterozygous)	F	No	AF(−)	...	56/0.13/0.08/0.424	...	No
8	Proband	55	*SCN1B* T189M (heterozygous)	F	No	Paroxysmal	55	65/0.18/0.08/0.420	30/65	No

AF indicates atrial fibrillation; EF, ejection fraction; F, female; LAD, left atrial diameter; and M, male.